

Quantitative analysis of phospholipids containing arachidonate and docosahexaenoate chains in microdissected regions of mouse brain^S

Paul H. Axelsen^{1,*} and Robert C. Murphy^{†,*}

Departments of Pharmacology, Biochemistry and Biophysics, and Medicine,* University of Pennsylvania School of Medicine, Philadelphia, PA, 19104-6084; and Department of Pharmacology,[†] Mail Stop 8303, University of Colorado at Denver Health Sciences Center, Aurora, CO 80045-0511

Abstract Phospholipids containing polyunsaturated fatty acyl chains are prevalent among brain lipids, and regional differences in acyl chain distribution appear to have both functional and pathological significance. A method is described in which the combined application of GC and multiple reaction monitoring (MRM) MS yielded precise relative quantitation and approximate absolute quantitation of lipid species containing a particular fatty acyl chain in milligram-sized tissue samples. The method uses targeted MRM to identify specific molecular species of glycerophosphocholine lipids, glycerophospho-ethanolamine lipids, glycerophosphoinositol lipids, glycerophosphoserine lipids, glycerophosphoglycerol lipids, and phosphatidic acids that contain esterified arachidonate (AA) and docosahexaenoate (DHA) separated during normal phase LC/MS/MS analysis. Quantitative analysis of the AA and DHA in the LC fractions is carried out using negative ion chemical ionization GC/MS and stable isotope dilution strategies. The method has been applied to assess the glycerophospholipid molecular species containing AA and DHA in microdissected samples of murine cerebral cortex and hippocampus. Results demonstrate the potential of this approach to identify regional differences in phospholipid concentration and reveal differences in specific phospholipid species between cortex and hippocampus. These differences may be related to the differential susceptibility of different brain regions to neurodegenerative disorders.—Axelsen, P. H., and R. C. Murphy. Quantitative analysis of phospholipids containing arachidonate and docosahexaenoate chains in microdissected regions of mouse brain. *J. Lipid Res.* 2010. 51: 660–671.

Supplementary key words plasmalogen • oxidative stress • normal-phase HPLC • negative-mode MS • Alzheimer's disease

This work was supported by grants from the NIA (AG20238), the American Health Assistance Foundation, and an Alzheimer's Association Zenith Fellows Award to PHA, and a large scale collaborative grant, Lipid Maps, GM069338 to RCM.

Manuscript received 1 September 2009 and in revised form 18 September 2009.

Published, JLR Papers in Press, September 18, 2009
DOI 10.1194/jlr.D001750

Brain is the most lipid-rich tissue in mammals, and lipid metabolism disorders often have prominent neurological manifestations. For example, it has been suggested that Alzheimer's disease (AD) is caused by a disorder of lipid metabolism, and this suggestion is supported by several general observations. One such observation is that elevated levels of lipid oxidation products are consistently found in AD (1). The oxidation products most closely associated with AD include various eicosanoids and chemically reactive aldehydes that are derived from arachidonic acid (AA) chains (2–6). In vitro studies have demonstrated that AA oxidation products may be produced by the action of amyloid β proteins on lipid membranes (7), and that these products in turn promote amyloid fibril formation (8–11).

Another general observation is that docosahexaenoic acid (DHA) levels are low in AD (12–15), and dietary DHA appears to be protective (16, 17). The neurological consequences of DHA deficiency (18) and the benefits of DHA intake (19–23) have also been demonstrated in mice, which have metabolic mechanisms to conserve and retain DHA during nutritional deficiency (24). However, not all models or protocols have found DHA to have a beneficial effect (25, 26). In contrast to the amyloidogenicity of an AA oxidation product, the corresponding oxidation product of DHA is not amyloidogenic (27).

An important step toward a deeper understanding of these observations is the development of means to quantify the phospholipid species containing AA and DHA

Abbreviations: AA, arachidonic acid or arachidonate; AD, Alzheimer's disease; CL, cardiolipin; DHA, docosahexaenoic acid or docosahexaenoate; MRM, multiple reaction monitoring; PA, phosphatidic acid; PC, phosphatidylcholine; PE, phosphatidylethanolamine; PG, phosphatidylglycerol; PI, phosphatidylinositol; PS, phosphatidylserine.

¹ To whom correspondence should be addressed.

e-mail: axe@upenn.edu (P.H.A.); Robert.Murphy@ucdenver.edu (R.C.M.)

^S The online version of this article (available at <http://www.jlr.org>) contains supplementary data in the form of one table.

chains in brain tissue. It is relatively easy to separate phospholipid classes by headgroup and quantify acyl chain content (28, 29), even in specific brain regions (30), but this approach does not resolve differences among lipid species that may be significant. Positive ion mass spectrometric analysis by headgroup provides quantitative precision and some resolution of species but cannot unambiguously identify species containing AA and DHA (31). Han et al. (32) described an internally standardized, negative mode MS approach for the analysis of phosphatidylethanolamine (PE) species in human and mouse brain, although the use of direct infusion and single-quadrupole analysis precluded unambiguous identification of species containing AA and DHA. A high-throughput procedure for quantifying plasmalogens in blood plasma by negative mode MS has also been described, although its sensitivity was not reported and it was designed to focus on only relatively few species (33).

This study was undertaken to develop a micro-scale method for identifying and quantifying polyunsaturated phospholipid molecular species and to document regional differences in brain tissue. Emphasis was placed on identifying concentration differences in adjacent brain regions that differ in function and in their susceptibility to the neurodegenerative processes associated with oxidative stress in AD.

MATERIALS AND METHODS

Key compounds and reagents

The following synthetic phospholipid standards were obtained from Avanti Polar Lipids (Alabaster, AB): 17:0a/20:4a-phosphatidylcholine (PC), 17:0a/20:4a-PE, 17:0a/20:4a-phosphatidylglycerol (PG), 17:0a/20:4a-phosphatidylinositol (PI), 17:0a/20:4a-phosphatidylserine (PS), 17:0a/20:4a-phosphatidic acid (PA), 21:0a/22:6a-PC, 21:0a/22:6a-PE, 21:0a/22:6a-PG, 21:0a/22:6a-PI, 21:0a/22:6a-PS, and 21:0a/22:6a-PA in methanol at concentrations ranging from 10 to 30 μ M, as well as (24:1)₃/14:1-cardiolipin (CL), (14:1)₃/15:1-CL, (15:0)₃/16:1-CL, and (22:1)₃/14:1-CL. Pentafluorobenzyl bromide and N,N-diisopropylethylamine were obtained from Sigma-Aldrich (St. Louis, MO). *d8*-AA and *d5*-DHA were obtained from Cayman Chemicals (Ann Arbor, MI). Neat AA and DHA for determining standard curves were obtained from NuCheck Prep Inc. (Elysian, MN).

Brain dissection

Three 9-month old 129S6/SVEV female mice (Taconic Farms, Inc., Hudson, NY) were euthanized by cervical dislocation. They were fed PMI type 5001 rodent chow ad libitum, and each mouse weighed approximately 20 g. Each brain was removed and frozen on dry ice within 5 min postmortem. Regions of interest were dissected from 1-mm-thick unstained coronal slices of mid-diencephalon while frozen under a dissecting microscope with the aid of a joystick micromanipulator (Eppendorf Transferman NK2, Westbury, NY). The two regions of interest in this work were the hippocampus (including dentate gyrus) and an adjacent portion of cerebral cortex of comparable size. One region was dissected from each brain hemisphere, yielding a total of six samples of hippocampus and six samples of cerebral cortex. Frozen tissue pieces were transferred to high-recovery clear borosilicate glass autosampler vials for weighing (9512S, Microsolv

Technology Corp., Eatontown, NJ). The mass of the dissected tissue samples ranged from 2.0 to 4.5 mg, and they were stored at -80°C for up to 1 month before processing. Other than a brief period during weighing, tissue samples continuously remained frozen in liquid nitrogen (-196°C), dry ice (-78°C), or a freezer (-80°C) until extracted.

Lipid isolation and chromatographic separation

Extraction was preceded by pulverizing the frozen samples in the bottom of the autosampler vial under liquid nitrogen with a Teflon pestle. Extraction was performed within the original vial using a modified Bligh-Dyer procedure. For tissue pieces from cerebral cortex and hippocampus (all weighing between 2.0 and 4.5 mg), a monophasic mixture of 400 μ l methanol, 200 μ l dichloromethane, and 160 μ l of 5 mM ammonium acetate was added to the ground tissue, and the sample was sonicated with a tip sonicator for 60 s. Another 200 μ l of dichloromethane and 160 μ l of water were added to this monophasic homogenate, along with 10 μ l/mg tissue of an internal standards mixture (see Table 1 for composition). This mixture was vortexed for 15 s, and the two resulting phases were clarified by brief low speed centrifugation. The lower phase (~ 350 μ l) was withdrawn and transferred to an autosampler vial with a PTFE lined cap (9532S, Microsolv Technology Corp., Eatontown, NJ) where it almost completely filled the vial. All extracts were kept at 5°C while in the autosampler awaiting analysis.

Aliquots (10 μ l) of each extract were injected onto a 4.6×250 mm silica column (Rx-SIL, Agilent), through which solvents were pumped at 1 ml/min. Solvent A was 30 parts hexanes and 40 parts isopropanol; solvent B was 30 parts hexanes, 40 parts isopropanol, and 7 parts 11 mM ammonium acetate in water. Solvent B was increased linearly from 30% to 98% over 10 min and was held at 98% for 15 min. The column was reequilibrated with 30% solvent B for at least 5 min before another sample was injected. Column effluent was directed into a high precision flow splitter (Analytical Scientific Instruments, El Sobrante, CA) with precisely 25% of the effluent directed into the standard ESI source for LC/MS/MS analysis and 75% collected in fractions for GC/MS analysis.

MS

Two multiple reaction monitoring (MRM) analytical methods were developed using an ABI 4000 QTrap mass spectrometer (Toronto, Canada). One method monitored a set of collision-induced mass transitions in the negative ion mode corresponding to the production of AA anions (m/z 303.2) from various phospholipid $[\text{M}-\text{H}]^{-}$ and $[\text{M}+\text{OAc}]^{-}$ anions, and the 17:0 heptadecanoate anions (m/z 269.2) derived from *sn1* chains in the AA-containing standards. The other method monitored the corresponding mass transitions for DHA anions (m/z 327.2) and 21:0 heneicosanoate anions (m/z 327.3). Each method divided the chromatographic separation into four periods, described below in detail. For all transitions, the dwell time was 100 ms, the source voltage was -4500 V, the collision voltage was -40 V, the collision gas was set to "medium", the resolution for both the first and third quadrupoles were set to "unit", and a drying gas at 300°C was applied to the spray. Transition peaks were integrated using Analyst 1.4.2 software, although all integrations were visually reviewed and many were adjusted manually.

GC/MS was performed with a 30-m ($30\text{-m} \times 0.2\text{-mm}$ inner diameter \times 0.25- μ m film thickness) ZB-1 polydimethylsiloxane capillary gas chromatograph column (Phenomenex, Torrance, CA) attached to a ThermoFinnigan (San Jose, CA) Trace DSQ mass spectrometer. The injector temperature was maintained at 230°C , and the transfer line was kept at 290°C . The mass spectrometric experiments were performed in negative CI mode (70 eV) with a

source temperature of 200°C. Helium was used as the carrier gas, with a constant flow rate of 0.8 ml/min. Phospholipid fractions for GC/MS analysis were saponified with 1 M NH₄OH, mixed with d8-AA and d5-DHA internal standards, esterified with pentafluorobenzyl bromide in N,N-diisopropylethylamine, and extracted into isooctane as described previously (34). A standard curve for converting the internal standard signals to concentration was prepared with solutions of neat AA and DHA in methanol that were derivatized in the same manner.

Data analysis

The integrated signal for each monitored mass transition was corrected for ¹³C content and processed as described in "Results." Quantitative sensitivity varied with the inherent difficulty of detecting lipid species in some headgroup classes and the amounts of these headgroup classes present in the brain. In addition, the results were subject to several assumptions that render them somewhat approximate. One assumption was that AA and DHA chains always occupied the *sn2* position, as in the synthetic standards. However, lipids may have these chains in the *sn1* position, they may have both an AA and a DHA chain, and they may even have two AA or two DHA chains. Precise corrections for these uncertainties are not available. When a lipid species has two AA or DHA chains, these species will be overcounted by a factor of $1 + r$, where r is an *sn1/sn2* ratio listed in Table 1. The numerical results provided for these species represent the measured values divided by this factor. No attempt was made to correct for differences in ionization efficiency due to differences in mass or due to differences between ether-linked and acyl-linked *sn1* chains.

RESULTS

Qualitative results: brain tissue

Simple mass spectra of brain tissue extracts are illustrated in Fig. 1. The positive ion scans in both brain regions were dominated by the $[M + H]^+$ ions of 16:0/18:1-PC (m/z 760.6), 16:0/16:0-PC (m/z 734.6), and 18:0/18:0-PC (m/z 790.6), as confirmed by separate MS/MS scans. The corresponding PE lipids were minor features of the spectrum (e.g., 16:0/18:1-PE at m/z 746.6). The most abundant PC lipids containing AA and DHA (e.g., 18:0/20:4-PC at m/z 810.6 and 18:0/22:6-PC at m/z 834.6) were also evident, but lipid species containing AA and DHA in any other headgroup classes could not be detected in the positive ion mode. The negative ion scans in both brain regions were dominated by the $[M - H]^-$ ions of 18:0/22:6-PS (m/z 834.5) and 18:0/20:4-PI (m/z 885.5). Some peaks, however, were most likely the superimposed ions of 18:0/22:6-PE and 18:0/18:0-PS, which were nearly isobaric at m/z 790.54 and 790.56, respectively.

Differences between brain regions were discernable in these spectra, but relatively few lipids containing AA or DHA could be positively or uniquely identified, and quantitative reproducibility was poor at this level of mass spectrometric analysis. Chromatographic separation of most any type would help overcome these problems by delivering lipid species at characteristic elution times and reducing ion suppression. Normal phase separation on a silica column was chosen for further studies, because tissue extracts could be injected without further processing and

lipid species with the same headgroup would elute at approximately the same times.

Quantitative results: synthetic standards

A mixture of 12 phospholipid standards was examined to characterize the elution characteristics of the silica column and normal phase solvent system. Based on the elution times of the major headgroup classes, the chromatography system described above in "Methods" was divided into four periods (Fig. 2): PG standards eluted in period 1 between 7.0 and 9.5 min; PI and PE standards eluted in period 2 between 8.5 and 11.5 min; PA and PS standards eluted in period 3 between 11.5 and 13.5 min; and PC standards eluted in period 4 between 18 and 19 min. For PC standards, the yield of *sn2* anions from $[M + OAc]^-$ ions was slightly greater than from $[M - CH_3]^-$ ions, so only the former were monitored.

To assess extraction efficiency, aliquots of the standard mixture were subjected to the extraction procedure described above, and transition signals corresponding to each standard species were measured in both the upper (aqueous) and lower (organic) phase. Results suggested that extraction efficiency was >88% in all cases, and >99% in all but 4 cases (Table 1).

The fatty acyl chains at the focus of this study, AA and DHA, are highly vulnerable to oxidative damage, so special precautions were taken to protect both synthetic standards and samples. These included grinding the samples under liquid nitrogen, the use of dichloromethane instead of chloroform to avoid exposure of lipids to phosphene, and a minimum of solution transfers. Transitions 16 and 32 Da greater than that of the AA and DHA standards (i.e., the monooxidized and peroxidized products) were monitored in the synthetic standard mixture and in brain. Only insignificant trace amounts were found.

To assess the suitability of the synthetic standards as internal standards for quantitative MS, a nominally equimolar mixture of the 12 standards was examined several times over a period of 4 weeks. This mixture was subjected to normal phase chromatography and MRM analysis as described above, and signal responses were corrected for ¹³C content. The fresh mixture yielded highly reproducible results and demonstrated that the AA-containing PE standard yielded 21.1-fold more signal than the AA-containing PI standard. Corresponding values for AA-containing PA and PS standards, as well as for the DHA-containing standards, are listed in Table 3.

Between analyses, the mixture was stored in plasma-cleaned autosampler vials at -80°C. After 4 weeks, the MRM transition signals were reexamined, and the signal responses from PG, PI, PE, PA, and PC standards were found to have decreased relative to the signals obtained for the PS standards. The losses ranged between 30% and 70%, with the greatest losses occurring in the PC standards. Losses of the PS standards were not assessed. Relative losses of similar magnitude were observed whether or not the vials had been plasma cleaned. The reason for these losses is not known but may involve the adherence of lipids in dilute solution to glass walls of the vial, glass-induced

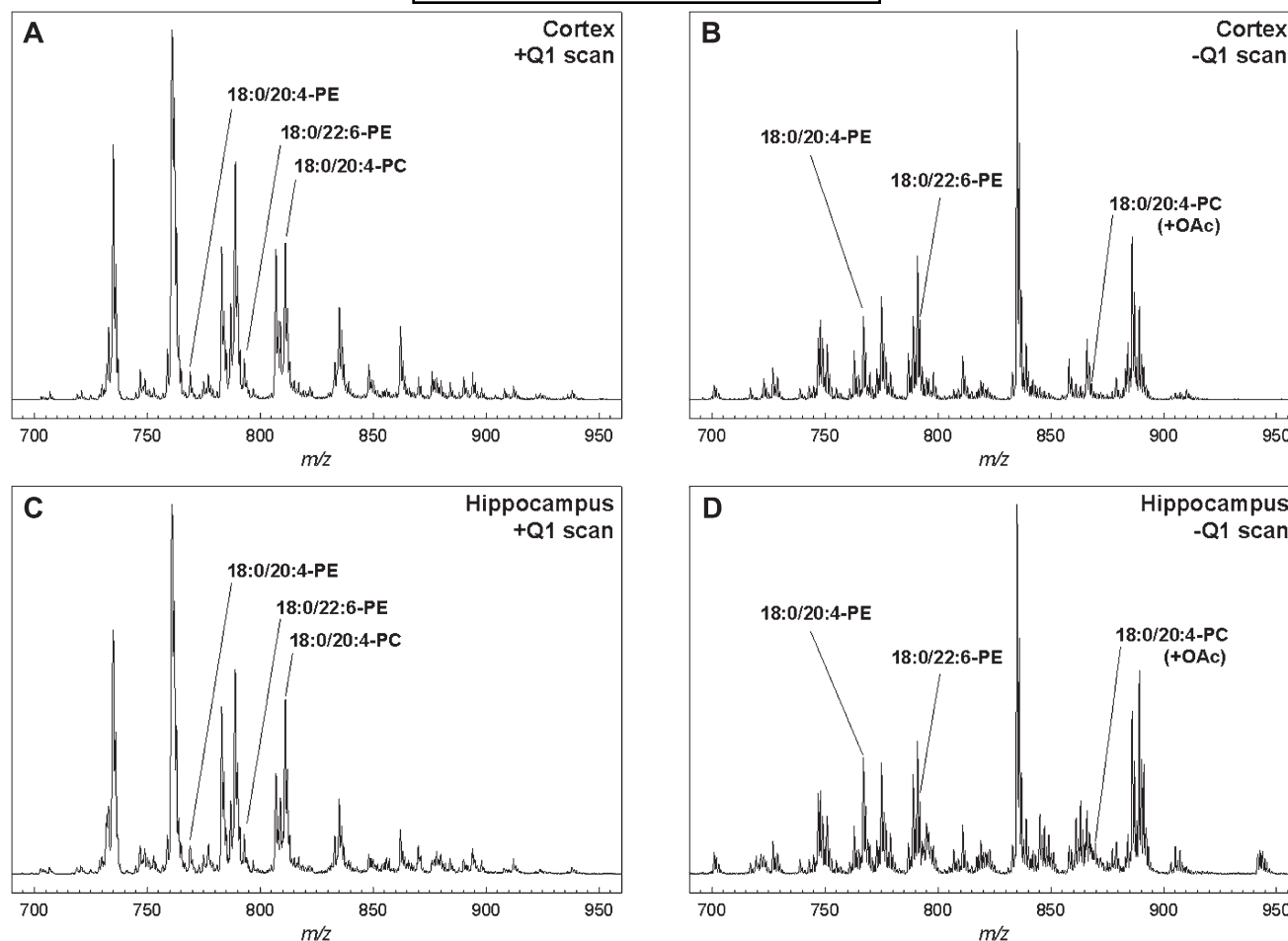


Fig. 1. Simple mass spectra obtained by direct injection of mouse brain extracts. Panels A and B are from cerebral cortex while panels C and D are from hippocampus. A and C are positive mode scans, while B and D are negative mode scans. Peaks corresponding to 18:0/20:4-PE, 18:0/22:6-PE, and 18:0/20:4-PC are labeled to show that even the most abundant lipids containing AA and DHA are often minor features in spectra of this type (see Figs. 5 and 6).

chemical decomposition, or oxidative damage. In any case, the losses precluded their use as reference standards. Nevertheless, they were useful as internal standards to correct for sample-sample variation.

Qualitative results: brain tissue

Extracts without added internal standards were initially examined with negative ion precursor scans for m/z 303.2 and m/z 327.3 ions to identify which molecular species containing AA and DHA, respectively, were present in the brain tissue, as well as to develop a list of mass spectral ion transitions for monitoring in the tandem mass spectrometer experiment. When a precursor ion peak eluted at a time characteristic of one headgroup and had a mass expected for a known phospholipid species bearing that headgroup, it was added to the list of monitored transitions for that headgroup class. The corresponding transition was also added to the list of monitored transitions for each of the other five headgroup classes. Ultimately, transitions for 27 individual species were monitored for each of the six AA-containing subclasses and for each of the six DHA-containing subclasses. Specific tandem mass spectrometric ion transitions are provided as supplementary Table I.

Brain extracts without internal standards were also examined for naturally occurring species with the same mass transitions as the internal standards. None of the transitions involving the collision-induced production of 17:0 heptadecanoate or 21:0 heneicosanoate anions from internal standard parent ions yielded measurable signal, but some of the transitions corresponding to AA and DHA anions from internal standards yielded significant peaks. Presumably, these peaks arose from phospholipids containing O-linked 18:0 and 22:0 *sn1* chains. Therefore, the expected signal for transitions yielding 20:4 and 22:6 chains from internal standards were calculated by dividing the signal obtained for transitions yielding 17:0 and 21:0 chains by the measured *sn1/sn2* ratios listed in Table 1. The differences between the calculated signal for transitions yielding 20:4 and 22:6 chains, and the measured signal for these transitions, were attributed to the corresponding O-linked species (these corrections were typically very minor).

The total ion chromatogram obtained by injecting approximately 3% (10 μ l) of the brain extract is shown in Fig. 2. The chromatogram was qualitatively similar whether transitions corresponding to AA-containing lipids or those corresponding to DHA-containing lipids were monitored,

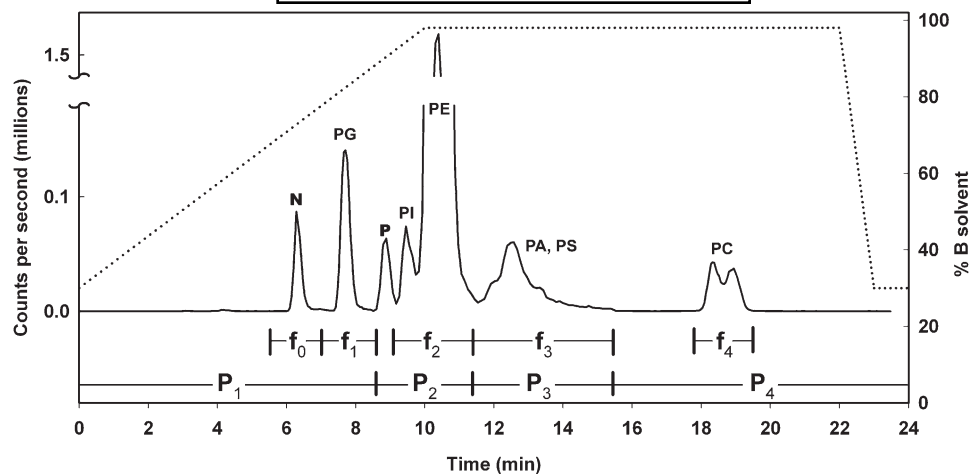


Fig. 2. Total ion chromatogram obtained by injecting a 10- μ l portion of a 350- μ l brain extract onto the silica column, and the MRM method for AA-containing lipids (solid trace, left axis). The MRM method for DHA-containing lipids is similar, with only a 10-s leftward temporal displacement. The solvent gradient is also shown (dotted trace, right axis). The method was divided into four periods indicated by intervals P₁ through P₄. During P₁ only PG transitions were monitored, and the peak is labeled 'PG'. During P₂, only PI and PE transitions were monitored and the peaks are labeled 'PI' and 'PE'. During P₃, only PA and PS transitions were monitored, and the broad overlapping peak is labeled 'PA, PS'. During P₄, only PC transitions were monitored and the split peak is labeled 'PC'. The peak labeled 'N' includes neutral lipids such as triglycerides and cholesteryl esters. The peak labeled 'P' is an unidentified polymer. Intervals over which the five fractions collected for GC/MS analysis are indicated by f₀ through f₄.

although DHA-containing lipids tended to elute 5–10 s before the corresponding AA-containing lipid. Signals arising from PG and PC lipids produced discrete peaks in periods 1 and 4, respectively. PI lipids produced a small peak at 9.5 min in period 2 that partially overlapped with a much larger peak produced by PE lipids at 11.0 min. This overlap did not obscure the identity of species yielding any given transition, however, because all PI species have greater masses than all PE species. Shallower solvent gradients were able to better resolve PI and PE lipids, but they lengthened the overall run, while the gradient illustrated was sufficient to alleviate ion suppression by PE lipids and maximize sensitivity for PI lipids.

PA and PS transitions coeluted over a broad interval in period 3. The ¹³C-isotopes in certain PA species could cause interference with the analysis of a PS species. For example, 20:0/20:4-PA and 20:0/22:6-PA have the potential for cross talk with the corresponding 14:1-containing PS species, while 22:0/20:4-PA and 22:0/22:6-PA have the potential for cross talk with the corresponding 16:1-containing PS species. Therefore, transitions corresponding

to PS lipids containing 14:1, 16:1, 20:0, and 22:0 chains were monitored to determine whether the signals recorded for the PS species required correction for cross talk from a ¹³C-containing PA species. In each case, the amount of cross talk was found to be negligible, due primarily to the low abundance of the PA species in question.

PG species produced narrow chromatographic peaks at 7.8 min (Figs. 2 and 3), but abundant signals at *m/z* 303.2 and 327.2 were also observed at ~6.3 min (Fig. 3C). The principle contributions to these earlier peaks were from parent ions with *m/z* 841.6 and 865.5. Negative mode product ion scanning confirmed that these were triglycerides containing 10:0/20:4/22:6 and 10:0/22:6/22:6 chains, while positive mode product ion scanning yielded no [M – 171]⁺ ions characteristic of the PG headgroup.

An unidentified polymeric material eluted at ~9.0 min, arising from a broad array of parent ions, and it produced a significant peak irrespective of whether PG species or PI species, or whether AA or DHA product ions were being monitored at that time. Product ion scanning of selected parent ions indicated that 303.2 and 327.2 fragments were

TABLE 1. Properties of the synthetic standards mixture, *sn1/sn2* ratios, and extraction efficiencies

AA Standard	Concentration* (nM)	<i>sn1/sn2</i> Ratio	Extraction Efficiency (%)**	DHA Standard	Concentration* (nM)	<i>sn1/sn2</i> Ratio	Extraction Efficiency (%)**
17:0/20:4-PC	221	0.37	100.0	21:0/22:6-PC	173	0.30	99.8
17:0/20:4-PE	10	0.38	88.1	21:0/22:6-PE	49	0.38	97.5
17:0/20:4-PG	12	0.33	99.6	21:0/22:6-PG	10	0.35	99.9
17:0/20:4-PI	19	0.56	100.0	21:0/22:6-PI	16	0.57	99.9
17:0/20:4-PS	107	2.24	94.5	21:0/22:6-PS	438	2.21	99.3
17:0/20:4-PA	113	3.15	100.0	21:0/22:6-PA	117	3.06	98.9

* The nominal concentration of each species, based on the manufacturer's label.

** Calculated as O/(A+O), where A and O are the transition signal recorded in the aqueous and organic phases, respectively.

TABLE 2. Fatty acid content by GC/MS in normal phase fractions

Fraction	Lipid Species	AA Content*		DHA Content*	
0	TG	1904	±262	828	±206
1	PG	78	±12	9	±3
2	PI,PE	5492	±898	6040	±1062
3	PA,PS	315	±48	1064	±236
4	PC	2490	±471	763	±129

* nmol/g tissue ± SD of 12 samples.

produced fortuitously through multiple fragmentations of larger ions.

Quantitative results: brain tissue

A total of six hippocampus and six cortical brain samples weighing between 2.0 and 4.5 mg were analyzed. The tissue pieces were reduced to 350- μ l extracts, each injection onto the column was 10 μ l, and precisely 25% of the column effluent was directed into the mass spectrometer. Therefore, the data was ultimately derived from 14–32 μ g of tissue. Each extract was injected twice, once for each of the two MRM methods, and each MRM analysis yielded 28 measurements (27 phospholipid species plus transitions arising from the 17:0 or 21:0 chains in the internal standards) for each of six phospholipid headgroup classes, or $6 \times 28 \times 2 = 336$ individual measurements.

The column effluent was collected in five fractions as indicated in Fig. 2. The AA and DHA content of each fraction were determined by GC/MS. Results grouped by brain region did not reveal significant differences between regions; therefore, GC/MS results for all 12 tissue samples were averaged and are listed in **Table 2**.

For PG and PC lipids, the conversion of MRM signals to quantitative results was performed by:

$$PL_n = r_{a,n} \left(\frac{FA_{x,w}}{r_{a,sum} \cdot 0.75 \cdot (10/350)} \right) \quad (1)$$

where PL_n is the average concentration of an individual phospholipid species n ,

$$r_{a,n} = \frac{1}{6} \sum_{i=1}^6 (c'_{a,n,i} / c'_{a,s,i}) \quad (2)$$

$$FA_{x,w} = \frac{1}{12} \sum_{i=1}^{12} (FA_{x,i} / w_i) \quad (3)$$

(averaged over all 12 samples)

$$r_{a,sum} = \frac{1}{12} \sum_{i=1}^{12} \sum_{n=1}^{28} r_{a,n,i} \quad (4)$$

(the sum of 28 transitions averaged over all 12 samples)

TABLE 3. Sensitivity ratios for MS/MS detection

Headgroup Classes	Lipids Containing AA	Lipids Containing DHA
PE / PI	21.1	61.7
PA / PS	3.3	6.1

$c'_{a,n,i}$ is the signal recorded for phospholipid species n in headgroup class a for sample i , and $c'_{a,s,i}$ is the signal recorded for an internal standard in the same headgroup class and sample. Primes indicates that the signal has been corrected for ^{13}C content, FA is the fatty acyl content of the collected column effluent fraction x for sample i in nmol, w is the mass of tissue sample i in g, 0.75 is the fraction of the column effluent that was collected by the fraction collector, and 10/350 is the portion of the tissue extract that was injected onto the column. It should be noted that the term in parentheses in equation 1 is constant for all phospholipid species within a headgroup class. Therefore, the relative values of PL_n for different sample sets depend only on the count ratio averages ($r_{a,n}$) and are independent of each other.

For PI/PE and PA/PS lipids, data reduction requires information about the relative sensitivity of the MRM method for these headgroup classes, given by the ratios s_{ab} of signals recorded from an equimolar mixture of a lipid in headgroup class a and a lipid in headgroup class b , provided in Table 3. Assuming that the sum of the signals recorded for all lipid species in a headgroup class, corrected for the sensitivity of the MRM method for lipids in that headgroup class, is proportional to the molar concentration of the lipids in that headgroup class, it follows that a fraction containing lipids in two different headgroup classes may be divided according to:

$$FA_a = FA_{x,w} \left(\frac{c_{a,tot}}{c_{a,tot} + s_{ab}c_{b,tot}} \right)$$

and

$$FA_b = FA_{x,w} \left(\frac{s_{ab}c_{b,tot}}{c_{a,tot} + s_{ab}c_{b,tot}} \right)$$

where

$$c_{a,tot} = \sum_{n=1}^{27} c'_{a,n}$$

and

$$c_{b,tot} = \sum_{n=1}^{27} c'_{b,n}$$

The concentration of an individual phospholipid may then be obtained by substituting either FA_a or FA_b for $FA_{x,w}$ in equation 1. This analytical approach has various strengths and potential weaknesses that will be discussed below. The one potential weakness we consider at this point is whether all of the AA and DHA chains in each fraction assayed by GC/MS were in phospholipids that corresponded to monitored MRM transitions. The two MRM lists included every fatty acyl chain with an even number of carbon atoms and every plausible number of double bonds, as well as known types of O-linked *sn*1 chains. Furthermore, the lists were compiled from precursor scans, thereby accounting for every detectable parent

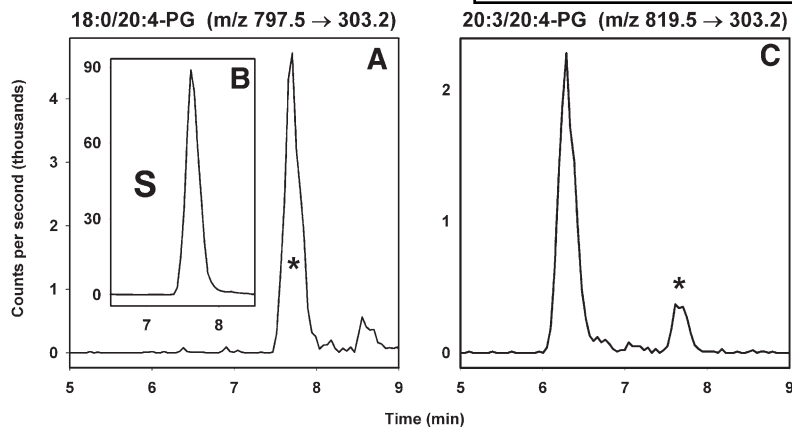


Fig. 3. Examples of extracted ion chromatograms for selected PG lipids. In panel A, the peak corresponding to 18:0/20:4-PG is shown eluting at 7.8 min, along with panel B as an inset showing that the synthetic standard 17:0/20:4-PG (labeled 'S') elutes at the same time. In panel C, the peak representing a minor species is also shown eluting at 7.8 min. The peak at 6.3 min is most likely an AA-containing triglyceride (e.g., 12:0/18:3/20:4-TG), because it coelutes with species shown by MS/MS analysis to represent 10:0/20:4/22:6-TG. The asterisk in panels A and C indicates that the parent ions also yield $[M-171]^+$ fragment ions in positive mode MS/MS studies.

ion yielding AA or DHA product ions. Precursor scans did detect AA and DHA in triglycerides, which eluted in fraction 0 and are included in Table 2. These scans did not detect any cholesterol esters of AA or DHA that would have also eluted in fraction 0, although these compounds ionize poorly. A targeted MRM method for lysophospholipids containing AA or DHA was created, and none were detected throughout the 24 min elution. Another targeted MRM method for lipids with PI-phosphate headgroups was created. Only trace amounts were detected, so no further attempt to quantify PI-phosphate lipids was made.

It has been reported that CLs in mouse brain tissue have a more diverse array of fatty acyl chains than those in myocardial or skeletal muscle tissue and that AA and DHA chains constitute a significant fraction of these chains (35). Therefore, we created a targeted MRM method for a set of synthetic CL standards and the mostly likely CL species based on the reported prevalence of fatty acyl chains in brain CLs. The method assumed that parent ions would be doubly charged. Results showed that synthetic CLs eluted at about the same time as PI and PE lipids. There were minimally detectable signals for several CL species, but they were insufficient for meaningful quantitation. These results are consistent with the low reported concentrations of AA and DHA in mouse brain CLs (4–10 nmol/mg protein) (35).

Results by headgroup class are summarized in Fig. 4. Overall, there were 10.3 $\mu\text{mol/g}$ tissue of AA-containing lipids in the tissue extracts, which was somewhat greater than the 8.7 $\mu\text{mol/g}$ of DHA-containing lipids. AA and DHA were most abundant in PE lipids but relatively rare in PG and PA lipids. Neutral, PI, and PC lipids contained more AA than DHA, while PE and PS lipids contained more DHA. The greater amount of DHA in PS lipids is consistent with the known preference for DHA chains among enzymes involved in PS headgroup synthesis (36).

Quantitative results for individual phospholipid species are summarized in Figs. 5 and 6. An important feature to note in these figures is the high degree of quantitative precision compared with the precision of the GC/MS fatty acid data listed in Table 2. Ordinarily, the uncertainty of the fatty acid quantitation would be propagated through the equations given above and reflected in the results for individual phospholipid species. However, this treatment

of the data would obscure the inherent precision of the MRM methods and the real differences in the amounts of individual phospholipid species in different brain regions. Therefore, none of the error in the GC/MS measurements was propagated through to the individual phospholipid results, and it should be understood that the relative quantitative precision with which brain regions may be compared is greater than the absolute quantitative precision. In other words, there is more uncertainty in the vertical scales for each graph than is suggested by the error bars, and this uncertainty may be derived from the data in Table 2.

Quantitative results: regional differences in brain tissue

As might be expected, the predominant species in most headgroup classes had 18:0 and 16:0 acyl-linked chains (Figs. 5 and 6). Most headgroup classes also had significant amounts of 18:1 chains, while the 20:4-PE and 22:6-PE

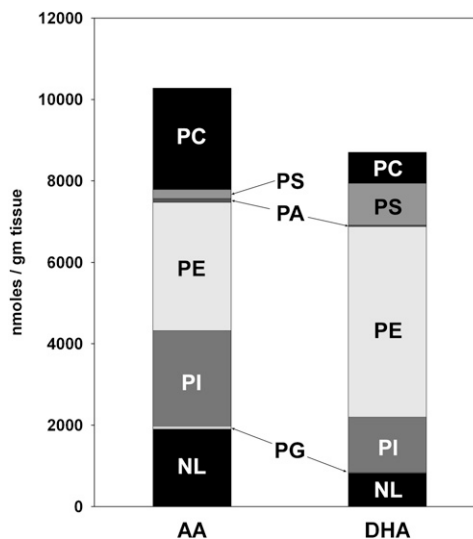


Fig. 4. Total AA and DHA in the six major headgroup classes and in neutral lipids. The data for neutral (NL), PG, and PC lipids were obtained directly from GC/MS analysis of fatty acyl chains in fractions f_0 , f_1 , and f_4 (see Fig. 1). The data for PI, PE, PA, and PS lipids were obtained by dividing the results from GC/MS analysis of fractions f_2 and f_3 as described in the text. There were no significant differences between cerebral cortex and hippocampus, so the results are the average of all 12 brain extracts.

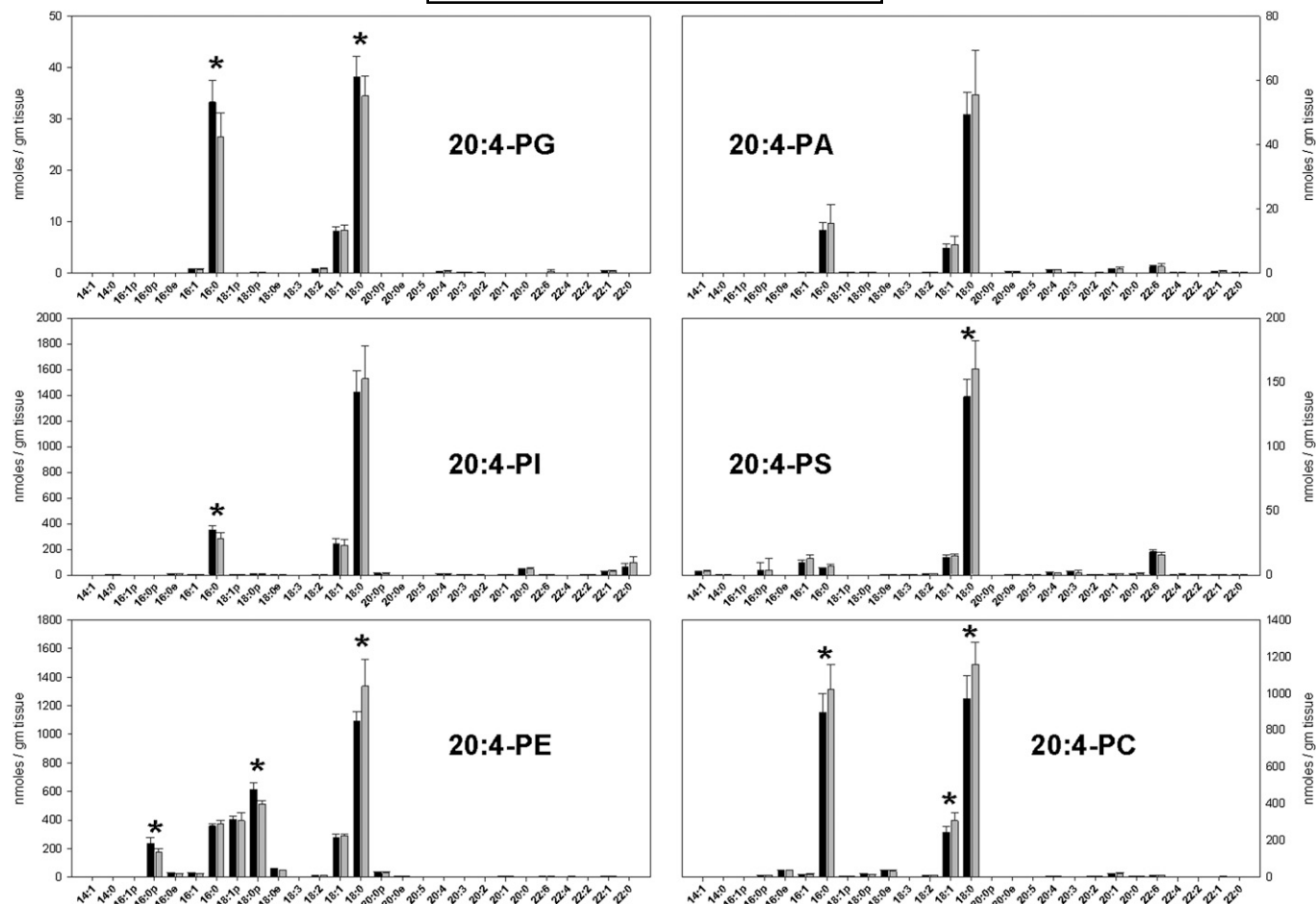


Fig. 5. The concentrations of AA-containing phospholipid species in cerebral cortex (black bars) and hippocampus (gray bars) in nmol/g tissue. Each result is the mean of six different brain extracts, and the error bars represent SD. An asterisk indicates results with statistically significant differences between brain regions. See text for information about the nature of quantitative uncertainty in these data.

subclasses also contained significant amounts of 16:0, 18:1, and 18:0 plasmalogens. The 22:6-PI subclass was notable for having an abundance of long saturated second acyl chains.

Among the AA-containing subclasses, the amount of 18:1/20:4 lipids was virtually identical in the two brain regions, except for a small difference in PC lipids. Cortical brain contained more 16:0/20:4-PG and 18:0/20:4-PG, as well as plasmalogens 16:0p/20:4-PE and 18:0p/20:4-PE, than hippocampus. Cortical brain contained less 18:0/20:4-PS, 18:0/20:4-PE, 16:0/20:4-PC, 18:1/20:4-PC, and 18:0/20:4-PC than hippocampus.

Among DHA-containing subclasses, all significant differences between brain regions reflected greater amounts in cortical brain. There were no significant differences detected in the 22:6-PA and 22:6-PE subclasses, but all major phospholipid species in the 22:6-PG, 22:6-PI, 22:6-PS, and 22:6-PC subclasses were significantly greater in cerebral cortex compared with hippocampus.

DISCUSSION

The results demonstrate that a large array of phospholipids may be quantified in milligram-sized samples of brain tissue and that the concentrations of specific lipid

species in such samples may be compared with a high degree of precision. Several factors contribute to this precision, beginning with a sample preparation protocol that emphasized ultracold tissue manipulations and the minimization of exposure to oxygen. These precautions are particularly important when focusing on polyunsaturated phospholipids because of their susceptibility to oxidative degradation. The addition of specific antioxidants may increase protection to these lipid species, but additives of this type were not included or examined in this study, because so-called antioxidants may also have pro-oxidant activity. Another factor that contributed to the precision of these measurements was the availability of synthetic odd-length internal standards for each headgroup and for each acyl chain type examined. The odd-length chains minimized spectral overlap with natural phospholipid species while coeluting with analytes under normal phase chromatographic conditions. Coelution of internal standards and analytes is advantageous, because it controls for varying degrees of ion suppression by other molecules that may be present in the eluent at any given time.

It should be noted that the relative phospholipid concentrations in the two different sample groups arise from independent measurements. This independence is achieved

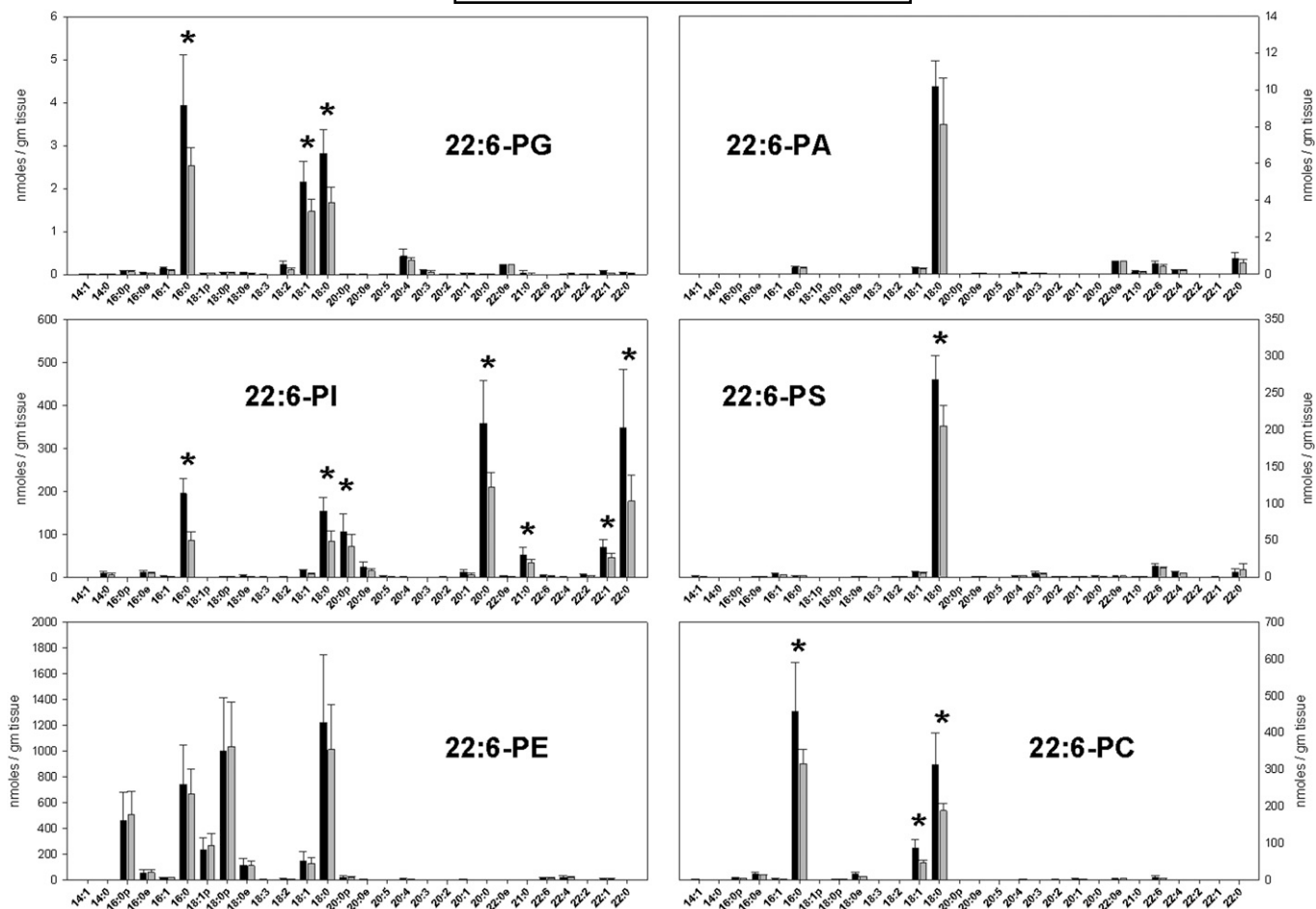


Fig. 6. The concentrations of DHA-containing phospholipid species in cerebral cortex (black bars) and hippocampus (gray bars) in nmol/g tissue. Each result is the mean of six different brain extracts, and the error bars represent SD. An asterisk indicates results with statistically significant differences between brain regions. See text for information about the nature of quantitative uncertainty in these data.

by averaging $r_{a,n}$ over the sample groups, but averaging the remaining terms (within the parentheses of equation 1) over all samples. It might appear reasonable instead to average $r_{a,n}/r_{a,sum}$ over each sample group and multiply those averages by the fatty acid content of each fraction. However, that approach either forces the total phospholipid content in different samples to be precisely equivalent or causes real differences between samples to be obscured by experimental uncertainty in the fatty acid content measurements. In contrast, the approach used in this work makes it reasonable to conclude, for example, that the two results for 18:1/20:4-PG in Fig. 5 are truly indistinguishable, while the results for 16:0/20:4-PG and 18:0/20:4-PG indicate that there is more AA-containing PG in cortex than in hippocampus.

The absolute scale on which we have placed these results is only approximately accurate, for several reasons, including numerical uncertainty in the fatty acid assay results, uncertainty in assigning the fatty acid assay results to lipids from different headgroup classes that coelute, and uncertainty over whether or not significant sources of AA and DHA other than phospholipid exist in each fraction. These problems could have been addressed in various ways, but addressing them would have solved only a small part of the more fundamental problem, the lack of avail-

able reference standards for the phospholipid species being examined. Without reference standards, it is necessary to assume that detection efficiency was constant within each headgroup class and that the ion signals recorded for each transition are proportional to the concentrations of the species present. Bruegger et al. (37) showed that detection efficiency in positive mode precursor scanning was a strong function of lipid mass, and a similar relationship may also apply to the negative mode approach used in this study. In addition, there are uncertainties about the ionization efficiency of *sn2* chains in phospholipids containing O-linked versus acyl-linked *sn1* chains, as well as differences in ion yields from the *sn1* and *sn2* positions (Table 1). Positional differences in ion yields will introduce error into any measurements in which AA and DHA do not occupy the *sn2* position as in the internal standard. There were measurable amounts of phospholipids containing two AA chains, two DHA chains, or one of each, so the potential for significant error exists. In situations where a phospholipid has one AA and one DHA chain, it is possible to calculate the fraction in which the AA chain is in the *sn1* position (see Appendix). The AA chain occupied the *sn1* position in 70–95% of such molecules in the PE, PA, and PS headgroup classes.

Precise relative quantities are of considerable value irrespective of uncertainty in the absolute quantities. As outlined above, such measurements are useful when investigating the role of altered brain lipid metabolism in disease states. For example, the data presented in Figs. 5 and 6 indicate that compared with cortical brain, the mouse hippocampus is relatively enriched in the most abundant species of AA-containing phospholipids, but relatively deficient in many species of DHA-containing phospholipids and AA-containing PE plasmalogens. These regional differences may reflect differences in the population of various cell types, such as the well-known enrichment of myelin in plasmalogens (38). Brain lipid content may also vary with gender, age, and stage of the estrous cycle in females. These factors were not examined in this work, nor was the distribution of lipid species in various organelle membranes (39), which may become apparent when subcellular fractions are examined. It is clear that the approach described herein would enable one to obtain precise results from the minute samples available for such studies.

The observation that PE plasmalogen concentrations are lower in the mouse hippocampus may be significant, because plasmalogen concentrations appear to be relatively low in AD brain (32, 40–42). Moreover, the region with relatively low plasmalogens concentrations, the hippocampus, tends to be affected by AD pathology earlier in the course of the disease (43). In a large population study, circulating plasmalogen levels were observed to decrease prior to the development of AD symptoms (33). Plasmalogens as a class are enriched in AA chains (38), and many investigators have suggested that plasmalogens have a protective role against oxidative damage (44–50) by virtue of their own particular susceptibility to oxidation (51). A vinyl ether group in the *sn1* position of a phospholipid increases the oxidative susceptibility of polyunsaturated AA chains at the *sn2* position (52–55).

On the other hand, plasmalogen deficiency may be a direct cause of neurological dysfunction. For example, decreased plasmalogens in a membrane appear to alter some measures of membrane stability (56), and the mobility of probes within hippocampal membranes increases in parallel with pathological involvement in AD (57). The cause of decreased plasmalogen levels, in turn, may be due to amyloid β protein exposure (58), and the consequences of such exposure may be the production of toxic oxidation products from the AA chain (7, 27, 59). Thus, it is not clear whether plasmalogens are consumed in the course of AD pathogenesis or are not present in sufficient quantities to exert an important protective role.

As with AA, plasmalogens are enriched in DHA chains and a vinyl ether group in the *sn1* position facilitates the oxidation of polyunsaturated chains in the *sn2* position (60). Phosphatidylserines are also enriched in DHA chains, because the enzymes that synthesize the PS headgroup prefer substrates containing DHA (36). The presence of DHA chains alters the distribution of AA-derived oxidation products (61). The significance of such findings in vivo is unknown, but they relate in an interesting way to in

vitro data showing that an AA oxidation product (hydroxynonenal) is amyloidogenic in vitro, whereas the analogous DHA oxidation product (hydroxyhexenal) is not (27). The available data on AA and DHA levels in the brain do not clarify whether they are reduced by oxidative degradation and their oxidation products lead to neurodegenerative disease, or whether reduced levels fail to protect other substances in the brain from oxidative damage. It is conceivable that the products of AA oxidation are neurotoxic and that the products of DHA oxidation are less toxic and, hence, protective.

In conclusion, a method has been developed to quantify phospholipid molecular species containing specific fatty acyl chains using targeted negative ion MRM-LC/MS/MS techniques. The relative abundance of these molecular species was used to convert the total amounts of AA and DHA in each HPLC fraction obtained by GC/MS into a quantitative assessment of each molecular species. The results of this study facilitate further study of polyunsaturated phospholipids in brain tissue and investigations into the functional and pathological significance of quantitative differences with methods that can distinguish among phospholipid species. **■**

Appendix: Analysis of acyl chain positions in phospholipid isomers containing both AA and DHA

Given two isomeric phospholipid species in a mixture bearing the same headgroup, one acyl-linked AA chain, and one acyl-linked DHA chain, we define k = a common proportionality constant. s = the fraction of the isomeric species in which $sn1$ = AA, i.e.,

$$s = \frac{[1-(AA)-2-(DHA)]}{[1-(AA)-2-(DHA)] + [1-(DHA)-2-(AA)]},$$

and $r = sn1/sn2$ (the yield ratio of *sn1* and *sn2* chains, given in Table 1).

Then, if the $I-(AA)-2-(DHA)$ molecules present in the sample produce ksr ions at $m/z = 303.2$, they should produce ks ions at $m/z = 327.2$, while the $I-(DHA)-2-(AA)$ molecules should produce $kr(I-s)$ ions at $m/z = 327.2$ and $k(I-s)$ ions at $m/z = 303.2$. Therefore, the total counts expected from the mixture for transitions yielding $m/z = 303.2$ (C_{AA}) and $m/z = 327.2$ (C_{DHA}), are given by

$$C_{AA} = k(1 + rs - s) \text{ and } C_{DHA} = k(r + s - rs).$$


TABLE 4. The fraction of lipid molecules containing both AA and DHA in which the AA chain is in position *sn1*

	Cortex	Hippocampus	Overall
PG	–	–	–
PI	–	–	–
PE	0.79	0.70	0.74
PA	0.95	0.95	0.95
PS	0.88	0.91	0.89
PC	–	–	–

–, Insufficient counts for this calculation.

Given measured values of r , C_{AA} , and C_{DHA} for any given headgroup, s may be calculated from

$$s = \left(\frac{C_{AA}}{C_{AA} + C_{DHA}} \right) \left(\frac{r+1}{r-1} \right) - \left(\frac{1}{r-1} \right)$$

With mean values of C_{AA} and C_{DHA} from the raw counts for each brain tissue sample, and values of r from Table 1, we obtained the values of s listed in Table 4. Among lipids with both an AA and a DHA chain, therefore, we conclude that the AA chain occupies the *sn*1 position in 70–90% of molecules in the PE, PA, and PS headgroup classes. 

REFERENCES

- Montine, T. J., M. D. Neely, J. F. Quinn, M. F. Beal, W. R. Markesbery, L. J. Roberts, and J. D. Morrow. 2002. Lipid peroxidation in aging brain and Alzheimer's disease. *Free Radic. Biol. Med.* **33**: 620–626.
- Pratico, D., V. M. Y. Lee, J. Q. Trojanowski, J. Rokach, and G. A. FitzGerald. 1998. Increased F-2-isoprostanes in Alzheimer's disease: evidence for enhanced lipid peroxidation in vivo. *FASEB J.* **12**: 1777–1783.
- Montine, T. J., K. S. Montine, W. McMahan, W. R. Markesbery, J. F. Quinn, and J. D. Morrow. 2005. F-2-isoprostanes in Alzheimer and other neurodegenerative diseases. *Antioxid. Redox Signal.* **7**: 269–275.
- Sayre, L. M., D. A. Zelasko, P. L. R. Harris, G. Perry, R. G. Salomon, and M. A. Smith. 1997. 4-hydroxynonenal-derived advanced lipid peroxidation end products are increased in Alzheimer's disease. *J. Neurochem.* **68**: 2092–2097.
- Ando, Y., T. Brannstrom, K. Uchida, N. Nyhlin, B. Nasman, O. Suhr, T. Yamashita, T. Olsson, M. El Sahly, M. Uchino, et al. 1998. Histochemical detection of 4-hydroxynonenal protein in Alzheimer amyloid. *J. Neurol. Sci.* **156**: 172–176.
- Markesbery, W. R., and M. A. Lovell. 1998. Four-Hydroxynonenal, a product of lipid peroxidation, is increased in the brain in Alzheimer's disease. *Neurobiol. Aging.* **19**: 33–36.
- Murray, I. V. J., M. E. Sindoni, and P. H. Axelsen. 2005. Promotion of oxidative lipid membrane damage by amyloid beta proteins. *Biochemistry.* **44**: 12606–12613.
- Koppaka, V., and P. H. Axelsen. 2000. Accelerated accumulation of amyloid beta proteins on oxidatively damaged lipid membranes. *Biochemistry.* **39**: 10011–10016.
- Koppaka, V., C. Paul, I. V. J. Murray, and P. H. Axelsen. 2003. Early synergy between Aβ42 and oxidatively damaged membranes in promoting amyloid fibril formation by Aβ40. *J. Biol. Chem.* **278**: 36277–36284.
- Komatsu, H., L. Liu, I. V. Murray, and P. H. Axelsen. 2007. A mechanistic link between oxidative stress and membrane mediated amyloidogenesis revealed by infrared spectroscopy. *Biochim Biophys Acta.* **1768**: 1913–1922.
- Murray, I. V. J., L. Liu, H. Komatsu, K. Uryu, G. Xiao, J. A. Lawson, and P. H. Axelsen. 2007. Membrane mediated amyloidogenesis and the promotion of oxidative lipid damage by amyloid beta proteins. *J. Biol. Chem.* **282**: 9335–9345.
- Kyle, D. J., E. Schaefer, G. Patton, and A. Beiser. 1999. Low serum docosahexaenoic acid is a significant risk factor for Alzheimer's dementia. *Lipids.* **34**: S245.
- Morris, M. C. 2006. Docosahexaenoic acid and Alzheimer disease. *Arch. Neurol.* **63**: 1527–1528.
- Schaefer, E. J., V. Bongard, A. S. Beiser, S. Lamon-Fava, S. J. Robins, R. Au, K. L. Tucker, D. J. Kyle, P. W. F. Wilson, and P. A. Wolf. 2006. Plasma phosphatidylcholine docosahexaenoic acid content and risk of dementia and Alzheimer disease - The Framingham heart study. *Arch. Neurol.* **63**: 1545–1550.
- Tully, A. M., H. M. Roche, R. Doyle, C. Fallon, I. Bruce, B. Lawlor, D. Coakley, and M. J. Gibney. 2003. Low serum cholesteryl ester-docosahexaenoic acid levels in Alzheimer's disease: a case-control study. *Br. J. Nutr.* **89**: 483–489.
- Morris, M. C., D. A. Evans, J. L. Bienias, C. C. Tangney, D. A. Bennett, R. S. Wilson, N. Aggarwal, and J. Schneider. 2003. Consumption of fish and n-3 fatty acids and risk of incident Alzheimer disease. *Arch. Neurol.* **60**: 940–946.
- Barberger-Gateau, P., C. Raffaitin, L. Letenneur, C. Berr, C. Tzourio, J. F. Dartigues, and A. Alperovitch. 2007. Dietary patterns and risk of dementia: the three-city cohort study. *Neurology.* **69**: 1921–1930.
- Calon, F., G. P. Lim, T. Morihara, F. S. Yang, O. Ubeda, N. Salem, S. A. Frautschy, and G. M. Cole. 2005. Dietary n-3 polyunsaturated fatty acid depletion activates caspases and decreases NMDA receptors in the brain of a transgenic mouse model of Alzheimer's disease. *Eur. J. Neurosci.* **22**: 617–626.
- Calon, F., G. P. Lim, F. S. Yang, T. Morihara, B. Teter, O. Ubeda, P. Rostaing, A. Triller, N. Salem, K. H. Ashe, et al. 2004. Docosahexaenoic acid protects from dendritic pathology in an Alzheimer's disease mouse model. *Neuron.* **43**: 633–645.
- Lim, G. P., F. Calon, T. Morihara, F. S. Yang, B. Teter, O. Ubeda, N. Salem, S. A. Frautschy, and G. M. Cole. 2005. A diet enriched with the omega-3 fatty acid docosahexaenoic acid reduces amyloid burden in an aged Alzheimer mouse model. *J. Neurosci.* **25**: 3032–3040.
- Calon, F., and G. Cole. 2007. Neuroprotective action of omega-3 polyunsaturated fatty acids against neurodegenerative diseases: evidence from animal studies. *Prostaglandins Leukot. Essent. Fatty Acids.* **77**: 287–293.
- Calderon, F., and H. Y. Kim. 2004. Docosahexaenoic acid promotes neurite growth in hippocampal neurons. *J. Neurochem.* **90**: 979–988.
- Green, K. N., H. Martinez-Coria, H. Khashwji, E. B. Hall, K. A. Yurko-Mauro, L. Ellis, and F. M. LaFerla. 2007. Dietary docosahexaenoic acid and docosapentaenoic acid ameliorate amyloid-beta and tau pathology via a mechanism involving presenilin 1 levels. *J. Neurosci.* **27**: 4385–4395.
- DeMar, J. C., K. Z. Ma, J. M. Bell, and S. I. Rapoport. 2004. Half-lives of docosahexaenoic acid in rat brain phospholipids are prolonged by 15 weeks of nutritional deprivation of n-3 polyunsaturated fatty acids. *J. Neurochem.* **91**: 1125–1137.
- Flouride, M., M. Fortier, M. Vandal, J. Tremblay-Mercier, E. Pleurmantle, M. Begin, F. Pifferi, and S. C. Cunnane. 2007. Unresolved issues in the link between docosahexaenoic acid and Alzheimer's disease. *Prostaglandins Leukot. Essent. Fatty Acids.* **77**: 301–308.
- Arendash, G. W., M. T. Jensen, N. Salem, N. Hussein, J. Cracchiolo, A. Dickson, R. Leighty, and H. Potter. 2007. A diet high in omega-3 fatty acids does not improve or protect cognitive performance in Alzheimer's transgenic mice. *Neuroscience.* **149**: 286–302.
- Liu, L., H. Komatsu, I. V. J. Murray, and P. H. Axelsen. 2008. Promotion of amyloid β protein misfolding and fibrillogenesis by a lipid oxidation product. *J. Mol. Biol.* **377**: 1236–1250.
- Yamamoto, A., and G. Rouser. 1973. Free fatty-acids of normal human whole brain at different ages. *J. Gerontol.* **28**: 140–142.
- Ulmann, L., V. Mimouni, S. Roux, R. Porsolt, and J. P. Poisson. 2001. Brain and hippocampus fatty acid composition in phospholipid classes of aged relative cognitive deficit rats. *Prostaglandins Leukot. Essent. Fatty Acids.* **64**: 189–195.
- Prasad, M. R., M. A. Lovell, M. Yatin, H. Dhillon, and W. R. Markesbery. 1998. Regional membrane phospholipid alterations in Alzheimer's disease. *Neurochem. Res.* **23**: 81–88.
- Rouzer, C. A., P. T. Ivanova, M. O. Byrne, H. A. Brown, and L. J. Marnett. 2007. Lipid profiling reveals glycerophospholipid remodeling in zymosan-stimulated macrophages. *Biochemistry.* **46**: 6026–6042.
- Han, X., D. M. Holtzman, and D. W. McKeel. 2001. Plasmalogen deficiency in early Alzheimer's disease subjects and in animal models: molecular characterization using electrospray ionization mass spectrometry. *J. Neurochem.* **77**: 1168–1180.
- Goodenowe, D. B., L. L. Cook, J. Liu, Y. Lu, D. A. Jayasinghe, P. W. K. Ahiahonu, D. Heath, Y. Yamazaki, J. Flax, K. F. Krenitsky, et al. 2007. Peripheral ethanolamine plasmalogen deficiency: a logical causative factor in Alzheimer's disease and dementia. *J. Lipid Res.* **48**: 2485–2498.
- Kayganich, K., and R. C. Murphy. 1991. Molecular-species analysis of arachidonate containing glycerophosphocholines by tandem mass-spectrometry. *J. Am. Soc. Mass Spectrom.* **2**: 45–54.
- Cheng, H., D. J. Mancuso, X. T. Jiang, S. P. Guan, J. Y. Yang, K. Yang, G. Sun, R. W. Gross, and X. L. Han. 2008. Shotgun lipidomics reveals the temporally dependent, highly diversified cardiolipin profile in the mammalian brain: Temporally coordinated postnatal diversification of cardiolipin molecular species with neuronal remodeling. *Biochemistry.* **47**: 5869–5880.
- Kim, H. Y. 2007. Novel metabolism of docosahexaenoic acid in neural cells. *J. Biol. Chem.* **282**: 18661–18665.

37. Brugger, B., G. Erben, R. Sandhoff, F. T. Wieland, and W. D. Lehmann. 1997. Quantitative analysis of biological membrane lipids at the low picomole level by nano-electrospray ionization tandem mass spectrometry. *Proc. Natl. Acad. Sci. USA*. **94**: 2339–2344.
38. Farooqui, A. A., and L. A. Horrocks. 2001. Plasmalogens: workhorse lipids of membranes in normal and injured neurons and glia. *Neuroscientist*. **7**: 232–245.
39. Jones, C. R., T. Arai, J. M. Bell, and S. I. Rapoport. 1996. Preferential in vivo incorporation of [³H]arachidonic acid from blood into rat brain synaptosomal fractions before and after cholinergic stimulation. *J. Neurochem*. **67**: 822–829.
40. Ginsberg, L., S. Rafique, J. H. Xuereb, S. I. Rapoport, and N. L. Gershfeld. 1995. Disease and anatomic specificity of ethanolamine plasmalogen deficiency in alzheimer's-disease brain. *Brain Res*. **698**: 223–226.
41. Farooqui, A. A., S. I. Rapoport, and L. A. Horrocks. 1997. Membrane phospholipid alterations in Alzheimer's disease: Deficiency of ethanolamine plasmalogens. *Neurochem. Res*. **22**: 523–527.
42. Guan, Z., Y. A. Wang, N. J. Cairns, P. L. Lantos, G. Dallner, and P. J. Sindelar. 1999. Decrease and structural modifications of phosphatidylethanolamine plasmalogen in the brain with Alzheimer disease. *J. Neuropathol. Exp. Neurol*. **58**: 740–747.
43. Eriksen, J. L., and C. G. Janus. 2007. Plaques, tangles, and memory loss in mouse models of neurodegeneration. *Behav. Genet*. **37**: 79–100.
44. Reiss, D., K. Beyer, and B. Engelmann. 1997. Delayed oxidative degradation of polyunsaturated diacyl phospholipids in the presence of plasmalogen phospholipids in vitro. *Biochem. J*. **323**: 807–814.
45. Hahnel, D., K. Beyer, and B. Engelmann. 1999. Inhibition of peroxyl radical-mediated lipid oxidation by plasmalogen phospholipids and alpha-tocopherol. *Free Radic. Biol. Med*. **27**: 1087–1094.
46. Hahnel, D., T. Huber, V. Kurze, K. Beyer, and B. Engelmann. 1999. Contribution of copper binding to the inhibition of lipid oxidation by plasmalogen phospholipids. *Biochem. J*. **340**: 377–383.
47. Maeba, R., Y. Sawada, H. Shimasaki, I. Takahashi, and N. Ueta. 2002. Ethanolamine plasmalogens protect cholesterol-rich liposomal membranes from oxidation caused by free radicals. *Chem. Phys. Lipids*. **120**: 145–151.
48. Maeba, R., and N. Ueta. 2003. Ethanolamine plasmalogens prevent the oxidation of cholesterol by reducing the oxidizability of cholesterol in phospholipid bilayers. *J. Lipid Res*. **44**: 164–171.
49. Morandat, S., M. Bortolato, G. Anker, A. Doutheau, M. Lagarde, J. P. Chauvet, and B. Roux. 2003. Plasmalogens protect unsaturated lipids against UV-induced oxidation in monolayer. *Biochim. Biophys. Acta.* **1616**: 137–146.
50. Kuczynski, B., and N. V. Reo. 2006. Evidence that plasmalogen is protective against oxidative stress in the rat brain. *Neurochem. Res*. **31**: 639–656.
51. Brosche, T., and D. Platt. 1998. Mini-review: the biological significance of plasmalogens in defense against oxidative damage. *Exp. Gerontol*. **33**: 363–369.
52. Khaselev, N., and R. C. Murphy. 1999. Susceptibility of plasmalogen glycerophosphoethanolamine lipids containing arachidonate to oxidative degradation. *Free Radic. Biol. Med*. **26**: 275–284.
53. Khaselev, N., and R. C. Murphy. 2000. Structural characterization of oxidized phospholipid products derived from arachidonate-containing plasmalogen glycerophosphocholine. *J. Lipid Res*. **41**: 564–572.
54. Khaselev, N., and R. C. Murphy. 2000. Peroxidation of arachidonate containing plasmalogen glycerophosphocholine: Facile oxidation of esterified arachidonate at carbon-5. *Free Radic. Biol. Med*. **29**: 620–632.
55. Murphy, R. C. 2001. Free-radical-induced oxidation of arachidonoyl plasmalogen phospholipids: Antioxidant mechanism and precursor pathway for bioactive eicosanoids. *Chem. Res. Toxicol*. **14**: 463–472.
56. Ginsberg, L., J. H. Xuereb, and N. L. Gershfeld. 1998. Membrane instability, plasmalogen content, and Alzheimer's disease. *J. Neurochem*. **70**: 2533–2538.
57. Zubenko, G. S. 1986. Hippocampal membrane alteration in Alzheimer's disease. *Brain Res*. **385**: 115–121.
58. Cheng, H., J. Xu, D. W. McKeel, and X. Han. 2003. Specificity and potential mechanism of sulfatide deficiency in Alzheimer's disease: an electrospray ionization mass spectrometric study. *Cell. Mol. Biol*. **49**: 809–818.
59. Murray, I. V. J., B. I. Giasson, S. M. Quinn, V. Koppaka, P. H. Axelsen, H. Ischiropoulos, J. Q. Trojanowski, and V. M. Y. Lee. 2003. Role of alpha-synuclein carboxy-terminus on fibril formation in vitro. *Biochemistry*. **42**: 8530–8540.
60. Zemski Berry, K. A., and R. C. Murphy. 2005. Free radical oxidation of plasmalogen glycerophosphocholine containing esterified docosahexaenoic acid: structure determination by mass spectrometry. *Antioxid. Redox Signal*. **7**: 157–169.
61. Davis, T. A., L. Gao, H. Yin, J. D. Morrow, and N. A. Porter. 2006. In vivo and in vitro lipid peroxidation of arachidonate esters: the effect of fish oil ω-3 lipids on product distribution. *J. Am. Chem. Soc*. **128**: 14897–14904.

ERRATA

A previously published errata in the September 2009 issue of the *Journal of Lipid Research* was incorrect. The authors of the article “Structural analysis of novel bioactive acylated sterol glucosides in pre-germinated brown rice bran” (*J. Lipid Res.* 49: 2188–2196) have advised the *Journal* that the notation $\Delta 8$ -cholesterol used in the original article is incorrect and the correct notation should be $\Delta 8(14)$ -cholestenol with the following structure: 5α -cholest-8(14)-en-3 β -ol based on “IUPAC-IUB Joint Commission on Biochemical Nomenclature: Nomenclature of Steroids” (*Pure & Appl. Chem.* 61: 1783–1822, 1989). This misspelling appeared online in the September 2009 issue but has since been corrected. The *Journal* sincerely regrets this error.

Please note that the correct structure is shown in Figure 3B as published in the original article.

DOI 10.1194/jlr.M800257ERR2

The authors of the article “Quantitative analysis of phospholipids containing arachidonate and docosahexaenoate chains in microdissected regions of mouse brain” (*J. Lipid Res.* 51: 660–671) have advised the *Journal* that “docosahexaenoate” had been misspelled as “docosahexenoate”. This misspelling appeared initially online but has since been corrected.

DOI 10.1194/jlr.D001750ERR